Application of a Secondary-Electron Transmission Monitor for High-Precision Intensity Measurements of Relativistic Heavy-Ion Beams

B. Jurado[1], K.-H. Schmidt, K.-H. Behr
Gesellschaft für Schwerionenforschung, Planckstraße 1, 64291 Darmstadt, Germany

Abstract: The application of a secondary-electron transmission monitor for high-precision intensity measurements of relativistic heavy-ion beams is investigated. The basic requirements, a strictly linear response as a function of beam intensity and a reliable absolute calibration are discussed on the basis of experimental data. Statistical fluctuations and systematic uncertainties of the calibration method are determined.

PACS: 29.40.-n; 29.40.CS.; 29.40.Mc; 29.40.Wk;
Keywords: Measurement of Heavy-Ion Beam Intensity; Secondary-Electron Transmission Monitor, Calibration Methods

1. Introduction

At relativistic energies, the usual method to determine heavy-ion beam intensities by measuring the electric current in a beam stop is not easily applicable due to the long range of charged secondary reaction products emerging from the stopping process. In this case, a SEcondary-Electron TRAnsmission Monitor (SEETRAM) which is based on the emission of secondary electrons from thin foils by the passage of the projectiles is a suitable device to survey the beam intensity almost without influencing the beam quality. Similar devices have been used at SATURNE [1] and CERN [2] to monitor the beam position and to measure the beam intensity. The present article reports on some properties of this detection method and discusses methods for its calibration, especially for lighter ions which emit only a small number of electrons. The present paper complements a previous publication [3] that investigated calibration methods for heavier ion beams.

2. The detector

The SEETRAM used at the Fragment Separator [4] at GSI Darmstadt consists of 3 titanium foils of 10 μm thickness and 11.5 cm in diameter that are mounted perpendicular to the beam, see figure 1a). While a former version of the SEETRAM was equipped with aluminium foils, titanium was chosen due to its higher long-term stability of the secondary-electron yield [5]. The outer foils are connected to a voltage of +80 V. The foils are curved in order to reduce the sensitivity to mechanical vibrations of the beam line. Secondary electrons emitted from the middle foil are collected by the two outer foils. A current integrator (CI), developed at GSI, measures the resulting positive current in the middle foil. A schematic view is depicted in 1b). The current integrator consists of

[1] This work forms part of the dissertation of B. Jurado ,Tel.: +49/6159/712727, FAX: +49/6159/712902, e-mail: b.jurado@gsi.de

several stages: Firstly, the input current is transformed into a voltage. An output signal of 1 Volt corresponds to a current that varies from 10^{-4} to 10^{-10} A, depending on the level of amplification (sensitivity) selected. There are seven different sensitivity steps that differ by factors of ten. The fast analogue output of this signal can be used as a monitor for measuring the extraction profile. Secondly, the signal passes two filters with time constants of 0.1 s and 1 s. The analogue output of the filtered signal is also available. Finally, the signal is digitised. The current integrator delivers an adjustable offset. As will be discussed in section 4.3, the noise signals are bipolar, thus it is important to tune the offset of the current integrator high enough to ensure that the digital outputs of the current integrator never stop. If this happens, any information on the magnitude of the current during this time is lost.

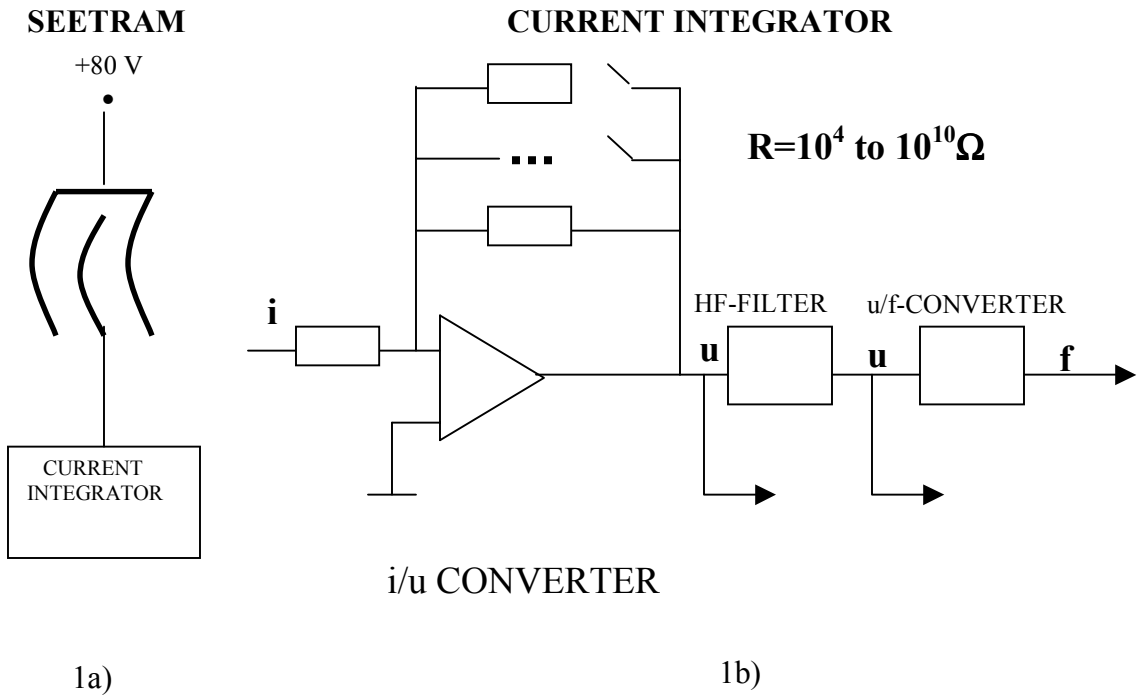

Figure 1: Schematic view of a) the SEcondary Electron TRAnsmission Monitor, SEETRAM, and b) the Current Integrator.

3. Linearity

When the SEETRAM is used for high-precision intensity measurements, needed for example for determining reaction cross sections, it is a basic requirement that the SEETRAM current is proportional to the intensity of the beam. At the heavy-ion synchrotron SIS18 at GSI, the current of the circulating beam can be measured by a fast beam transformer [6]. Assuming that the extraction efficiency does not depend on the beam current, the linearity of the SEETRAM current as a function of the beam intensity can be verified. Figure 2 shows the current in the SEETRAM, measured after extraction

at the target position of the fragment separator, as a function of the circulating beam intensity. The measurement was performed with a lead beam of 500 *A* MeV. The relative rms deviations from the linear fit amount to $17 \cdot 10^{-14}$A so that we can assume a strict proportionality between the SEETRAM current and the beam current. More over, up to the highest beam intensities available at the moment of the measurement, no saturation effect could be observed.

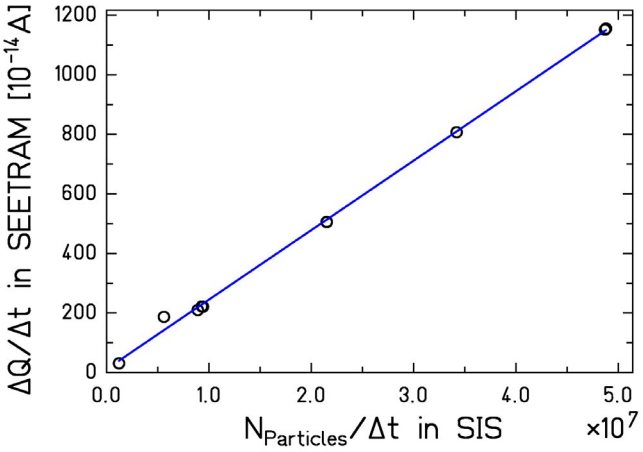

Figure 2: Electric current measured with the SEETRAM at the FRS as a function of the absolute intensity in SIS for a lead beam of 500 *A* MeV. Δt corresponds to a spill length of 5 s. The open points represent the experimental data and the solid line the linear fit. The SEETRAM was equipped with aluminium foils.

4. Calibration

4.1. General considerations

Since the number of electrons recorded by the SEETRAM depends on the nature and the energy of the projectile [7, 8], absolute beam-intensity measurements require a calibration of the detector. In the most direct method, one may compare the accumulated SEETRAM current with the number of particles counted with a fast detector such as a scintillation detector (SCI), see [9]. However, this method has several limitations and drawbacks. Firstly, fast plastic scintillators are subject to radiation damages when they are hit by high-intensity beams. This makes the method difficult to be used in a standard application. Secondly, the number of electrons ejected by low-*Z* projectiles from the SEETRAM foil is quite low. As a consequence, accurate particle counting at very high rates is required. Considering fluctuations in the offset current of the current integrator, intensities higher than the saturation limit of the SCI are needed for ions with $Z < 40$ in order to produce a current in the SEETRAM that can be measured with sufficient precision. Due to our experimental conditions (isolation of the detector, cable lengths, etc.) and the accuracy needed, the saturation limit of the SCI is 10^5 particles per second.

For counting rates below this limit, the saturation effects in the SCI are smaller than 1%. By improving the experimental conditions, the saturation limit might be somewhat increased, but in any case, the method is not applicable for the lightest projectiles.

A solution of these problems by using a self-calibrating ionisation chamber (IC) is described in ref. [3]. The IC delivers a particle-counting signal and a current signal that both are proportional to the beam intensity. The IC current is about 1000 times higher than the SEETRAM current, overlapping in the low-intensity region with the particle counting and in the high-intensity region with the SEETRAM current. Nevertheless, the lighter the charge of the ions, the more difficult it is to resolve the single-particle pulses of the IC from the electronic noise. In the best case, this noise corresponds to an energy loss in the counting gas of the IC of the order of 50 keV. To clearly distinguish the pulses from this background, the energy-loss signals should be at least one order of magnitude higher. An additional uncertainty is introduced by the fluctuations of the energy-loss signals that cause an overlap of the particle signal with the noise. In order to decide whether the IC can be used for counting light ions, it is necessary to carefully analyse the energy-loss signals and find out if they can be discriminated against the noise. From these considerations, one expects that particle counting with the IC is not suitable for ions with $Z < 10$. Hence, for such cases the particle counting should be performed with a SCI. But still the IC is needed to provide a broad region of overlap between the particle counting of the SCI and the SEETRAM. In the following, we will describe an experiment with a ^{12}C beam at 195 *A* MeV. In this case, a counting rate of at least $1.7 \cdot 10^6$ particles per second in the SCI would be needed to achieve an adequate overlap with the usable current signals of the SEETRAM. This counting rate is already beyond the saturation limit of the SCI. However, by using the IC the rates to be recorded with the SCI are lowered by three orders of magnitude.

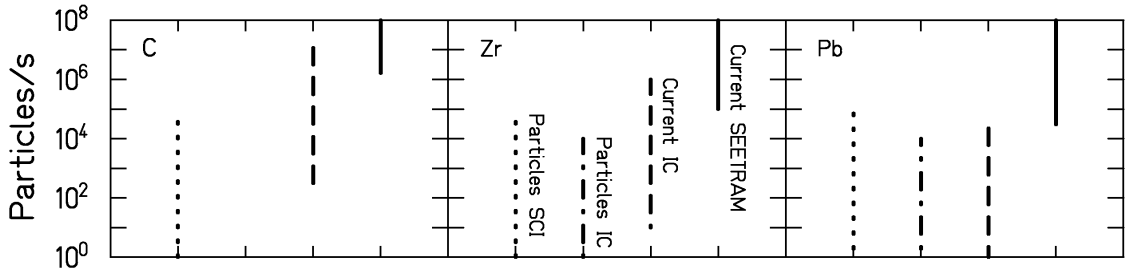

Figure 3: The ranges of operation of the SEETRAM (solid line), of the IC current (dashed line), of the IC particle counting (dashed-dotted line) and of the SCI (dotted line) are represented for carbon, zirconium and lead ions at 1 *A* GeV. In any case, the IC current provides on the one hand a good overlap to particle counting with the SCI or the IC and to the SEETRAM current on the other hand. For carbon ions, the IC signal is too low to be used for particle counting.

In figure 3, the operation range of the different detectors is represented for carbon, zirconium and lead ions at 1 *A* GeV. As mentioned above, the scintillator has an upper

limit due to saturation. The SEETRAM has a lower limit of 10^{-12} A in order to produce a secondary-electron current that is high enough to be distinguished from the offset with an accuracy better than 1%. This lower limit is also valid for the IC current signal that in addition has an upper limit of 10^{-7} A due to recombination effects, see section 4.2.The figure shows that for heavy ions like lead, particle counting with the SCI directly overlaps with the SEETRAM current. However, for lower charges the overlapping region decreases, since the intensity needed to overcome the offset uncertainty in the SEETRAM increases. The limiting case occurs for zirconium, for lighter ions like carbon there is no overlap, and this method is no longer applicable with the desired accuracy. In this case, the current signal of the IC provides the necessary overlap between the secondary-electron current and the particle counting, which is provided by the SCI since the signals in the IC are too low to be used for particle counting below $Z = 10$.

4.2. Experiment

In the present work, we report on a calibration of the SEETRAM for 195 MeV ^{12}C ions. As discussed in the previous section, this is a difficult case, since it requires an appropriate operation of the SCI and the IC. A first part of the calibration was done at high intensities where the SEETRAM current was calibrated against the IC current. For these high intensities we operated the current integrator of the IC at rather low sensitivity of 10^{-11} As per output pulse, while the current integrator of the SEETRAM was operated with the highest sensitivity of 10^{-14} As per output pulse. One should not forget that the beam intensity is constrained by the condition that the current in the IC should not exceed 10^{-7} A, since for higher currents recombination effects in the IC cannot easily be corrected**.**

Figure 4 shows several spills as measured by the SEETRAM together with the corresponding spills as measured by the IC. The spill length was 5 s.

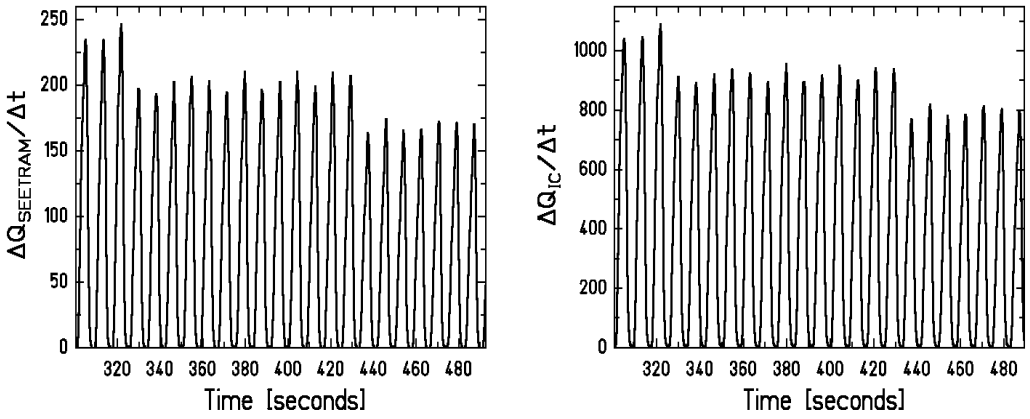

Figure 4: The left figure represents the accelerator spills measured by the SEETRAM. The right figure shows the same spills measured by the IC. $\Delta Q_{SEETRAM}$ is measured in units of 10^{-14} As, ΔQ_{IC} in units of 10^{-11} As. The time unit is $\Delta t = 100$ ms.

After subtracting the offset and integrating the charge in the SEETRAM and in the IC separately over the different spills, we plot the results of the integration obtained for the IC against the ones obtained for the SEETRAM in figure 5.

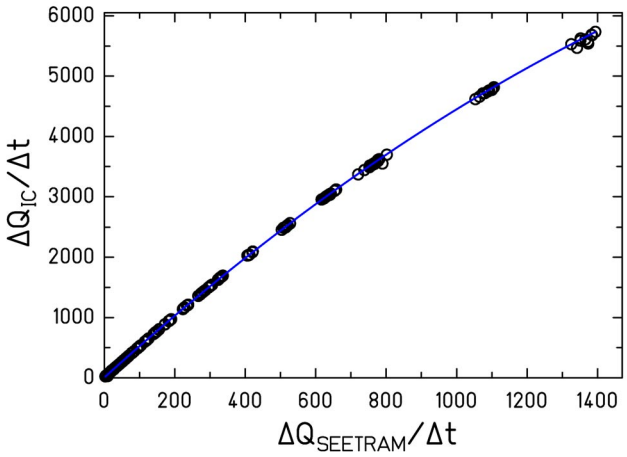

Figure 5: IC current versus secondary-electron current in the SEETRAM. $\Delta Q_{SEETRAM}$ is measured in units of 10^{-14} As, ΔQ_{IC} in units of 10^{-11} As. The time unit is $\Delta t = 5$ s which corresponds to the spill length. The circles represent the experimental data; the solid line represents the parabolic fit.

As the beam intensity increases, the current in the IC is affected by recombination losses. Recombination is proportional to the product of the density of gas ions and the density of electrons inside the chamber. Since each of them is proportional to the beam intensity, recombination effects can be considered in the analysis by fitting a second-order polynomial to the ionisation current as a function of the SEETRAM current.

$$I_{IC} = F_2 \cdot I_{SEETRAM}^2 + F_1 \cdot I_{SEETRAM} + F_0 \qquad (1)$$

with $F_2 = -8.521 \cdot 10^{13}$ A^{-1}, $F_1 = 5297$ and $F_0 = 5.347 \cdot 10^{-11}$ A. Note that expression (1) contains also a zero-order term F_0. We included this coefficient because, as can be seen from figure 4, in this measurement the offset of the SEETRAM was not positive, and it could not be subtracted. In this way, this term is determined by the fit. This additional fit parameter enhances the error of the fit but does not change the value of the coefficients. The calibration factor for the IC current per SEETRAM current is given by the first-order coefficient of the parabolic fit.

$$F_{IC\text{-}SEETRAM} = \frac{I_{IC}}{I_{SEETRAM}} = 5297 \pm 5$$

Note that the second-order coefficient allows extending the fit into the region of sizeable recombination effects.

To determine the number of particles that correspond to each SEETRAM output signal, i.e., to determine the SEETRAM calibration factor, we still need to calibrate the IC current against the SCI particle counting. This part of the calibration was performed at low intensities in order to avoid any saturation of the SCI. Consequently, the sensitivity of the IC integrator was increased to 10^{-14} As per output pulse. The spills measured by the SCI for diverse intensities and the corresponding spills from the IC current are shown in figure 6.

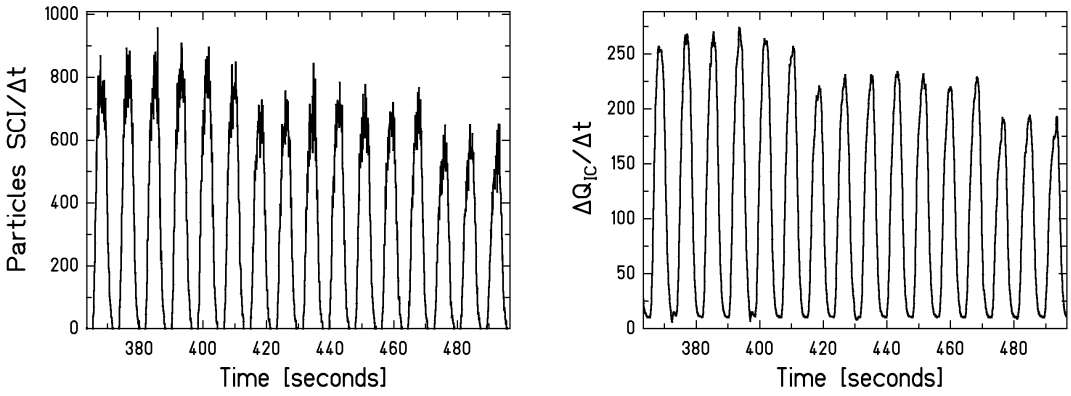

Figure 6: The left figure represents the accelerator spills as measured by the SCI, and the right figure the same spills as measured by the IC. ΔQ_{IC} in units of 10^{-14} As. The time unit is Δt = 100 ms.

After subtracting the offset of the IC and integrating the different spills, we represent the ions per spill measured by the SCI against the corresponding charge per spill collected by the IC, this is shown in figure 7. The linear fit gives the calibration factor of the charge produced in the IC per particle.

$$F_{IC-Particles} = (0.3204 \pm 0.0003) \cdot 10^{-14} \frac{\text{As}}{\text{particle}}$$

From the two calibration factors we obtain the final SEETRAM calibration factor:

$$F_{SEETRAM} = \frac{F_{IC-SEETRAM}}{F_{IC-Particles}} = 1.652 \cdot 10^{18} \frac{\text{particles}}{\text{As}}$$

$F_{SEETRAM}$ represents the number of ^{12}C ions needed to produce one unit of electric charge collected from the SEETRAM. The value of $F_{SEETRAM}$ observed previously in refs. [10,11] for this beam in a SEETRAM with aluminium foils was $1.38 \cdot 10^{18}$ particles/As. This value is about 17% lower than the value that we have obtained. Similar differences have already been observed in previous calibrations with different projectiles. They are most probably due to the fact that, as discussed in [5], the secondary emission from aluminium foils tends to decrease up to 50% after a long-term use in the region where the beam impinges. Such decrease of the secondary-electron efficiency in the impact region of the aluminium foils has also been observed at GSI [12].

Finally, we give the relative statistical error of the calibration as determined from the deviation of the data points in figures 5 and 7:

$$\frac{\sigma_{F\_SEETRAM}}{F_{SEETRAM}} = \sqrt{\left(\frac{\sigma_{F\_IC\_SEETRAM}}{F_{IC\_SEETRAM}}\right)^2 + \left(\frac{\sigma_{F\_IC\_particles}}{F_{IC\_particles}}\right)^2} = 1.4 \cdot 10^{-3}$$

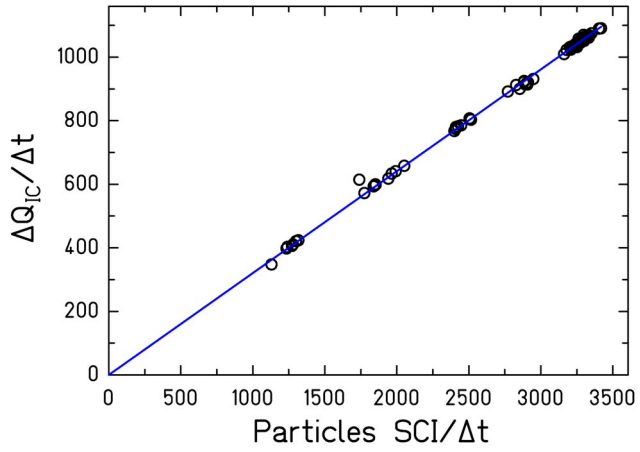

Figure 7: IC current per spill versus number of particles per spill detected by the SCI. ΔQ_{IC} is measured in units of 10^{-14} As and Δt = 5 s. The circles represent the experimental data; the solid line represents the linear fit.

This value is remarkably small. It results if the reduced Chi-squared of the linear respectively parabolic fit is required to be unity. To understand the value, we should consider that the inherent statistical fluctuations of the method are given by the fluctuations of the accumulated number of secondary-electrons and the accumulated ionisation charge, respectively, for a given number of projectiles. Due to the large number of ions comprised in one spill, this fluctuation is extremely small. The fluctuations observed in the data points are rather due to shortcomings of the data analysis, e.g. in extracting the signals from the dark current of the current integrator. These effects will be discussed in next section.

4.3. Offset and systematic errors

The offset of the current integrator of the IC presents a complicated structure, especially for the lower-intensity part of the calibration. In figure 8, the bipolar signals of the noise can be clearly distinguished. Note that any noise signal e.g. by a varying electric or magnetic field at the detector or along the cables is bipolar as long as there is good electric isolation. These bipolar noise signals are apparently connected to the extraction procedure of the SIS beam, since the distance between the bipolar signal and the next

inverse signal is about 5 s, i.e. the actually used spill length. We assume that the SEETRAM is sensitive to the high-voltage pulses applied to the extraction septum. Since the integral of the bipolar signals is zero, and the signals come regularly, the remaining effect of these signals in the calibration is zero on the average, provided that both parts of the bipolar signals are included in the analysis.

In the calibration procedure described above, there are different sources of systematic errors. Firstly, one has to take care that the different sensitivity ranges of the current integrator are carefully adjusted, since the calibration relies on combining the results obtained in different ranges. Additional sources of systematic errors are irregular spill shapes that lead to fluctuating recombination losses at higher intensities where the ionisation current is affected by recombination effects. Finally, an important error is introduced by the uncertainty in subtracting the offset. We estimate that the error induced by these effects is not larger than 2 % in the present experiment. This should be a typical value for the method which is expected to be generally valid for other applications if the analysis is carefully done.

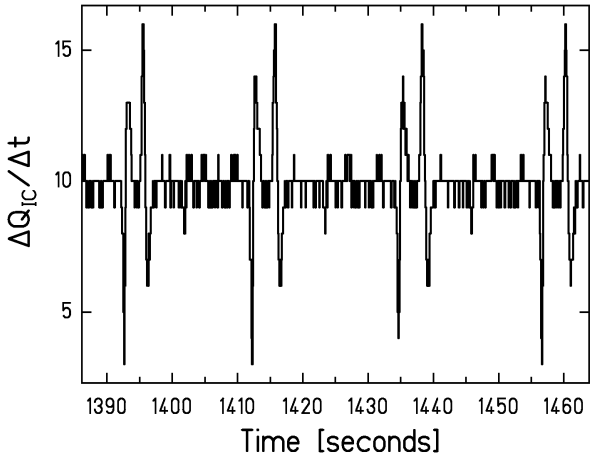

Figure 8: Offset in the IC when it is operated at the lowest sensitivity. Δt = 100 ms. The bipolar noise signals can be clearly observed.

5. Conclusion

The secondary-electron transmission monitor has proven to be a reliable tool for determining the beam dose in high-precision experiments with relativistic heavy ions. Its current was found to be strictly proportional to the beam intensity without showing any saturation effect. The calibration procedure for light ions was made by using an ionisation chamber. Since the current produced in the ionisation chamber is many orders of magnitude higher than the current produced in the secondary-electron transmission

monitor, the particle counting can be performed at considerably lower rates allowing for much more reliable calibrations.

Acknowledgment: We thank the (GSI-)S236-Kollaboration for their assistance during the measurement.

---

[1] R. Anne, A. Lefol, G. Milleret, R. Perret, Nucl. Instrum. Methods 152 (1985) 395
[2] K. Bernier, G. de Rijk, G. Ferioli, E. Hatziangeli, A. Marchionni, V. Palladino, G.R. Stevenson, T. Tabarelli de Fatis, E. Tsesmelis, CERN Report 97-07, 3 July 1997
[3] A. Junghans, H.-G. Clerc , A. Grewe, M. de Jong, J. Müller, K.-H. Schmidt, Nucl. Instrum. Methods A 370 (1996) 312
[4] H. Geissel, P. Armbruster, K.-H. Behr, A. Brünle, K. Burkard, M. Chen, H. Folger, B. Franczak, H. Keller, O. Klepper, B. Langenbeck, F. Nickel, E. Pfeng, M. Pfützner, E. Roeckl, K. Rykaczewsky, I. Schall, D. Schardt, C. Scheidenberger, K.-H. Schmidt, A. Schröter, T. Schwab, K. Sümmerer, M. Weber, G. Münzenberg, T. Brohm, H.-G. Clerc, M. Fauerbach, J.-J. Gaimard, A. Grewe, E. Hanelt, B. Knödler, M. Steiner, B. Voss, J. Weckenmann, C. Ziegler, A. Magel, H. Wollnik, J.-P. Dufour, Y. Fujita, D. J. Vieira, B. Sherrill, Nucl. Instrum. Methods B 70 (1992) 286
[5] G. Ferioli, R. Jung, CERN Report, Contribution to the Third European Workshop on Beam Diagnostics and Instrumentation for Particle Accelerators (DIPAC 97) October 1997
[6] H. Reeg, N. Schneider, S. Steinhäuser, GSI Scientific Report 1990, page 392
[7] E. J. Sternglass, Phys. Rev. 108 (1957) 1
[8] A. Albert, K. Kroneberger, O. Heil, K. O. Groneveld, H. Geissel, Nucl. Instrum. Methods A 317 (1992) 397
[9] http://www-wnt.gsi.de/kschmidt/seetraminfo/SEETRAM.html
[10] C. Ziegler, Diploma Thesis, Institut für Kernphysik, TH Darmstadt (1992)
[11] T. Brohm, Ph. D. Thesis, Institut für Kernphysik, TH Darmstadt (1994)
[12] K. Sümmerer, private communication